American Mineralogist, Volume 89, pages 455–461, 2004

A new dense silica polymorph: A possible link between tetrahedrally and octahedrally coordinated silica

SHENG-NIAN LUO,[1,4] OLIVER TSCHAUNE,[1,2,*] PAUL D. ASIMOW,[3] AND THOMAS J. AHRENS[1]

[1]Lindhurst Laboratory of Experimental Geophysics, Seismological Laboratory, California Institute of Technology, Pasadena, California 91125, U.S.A.
[2]High Pressure Science and Engineering Center and Department of Physics, University of Nevada, Las Vegas, Nevada 89154-4002, U.S.A.
[3]Division of Geological & Planetary Sciences, California Institute of Technology, Pasadena, California 91125, U.S.A.
[4]Plasma Physics (P-24) and Earth and Environmental Sciences (EES-11), Los Alamos National Laboratory, Los Alamos, New Mexico 87545, U.S.A.

ABSTRACT

We present the discovery of a novel dense silica polymorph retrieved from shock-wave and diamond-anvil cell experiments. This polymorph is the first observed silicate composed of face-sharing polyhedra and it has a density similar to stishovite. Sterical constraints on the bond angles induce an intrinsic disorder of Si positions, such that the Si-coordination is transitional between four- and sixfold. The structure provides a mechanism for this coordination change in silica and other silicates at high temperature that is fundamentally different from mechanisms at 300 K. The new polymorph also illustrates how the face-sharing polyhedra, naturally occurring along previously proposed compression mechanisms for dense silicate melts, can be constructed without inferring unphysically small bond angles.

INTRODUCTION

The transition from tetrahedral to octahedral coordination of Si cations by O anions is the dominant structural change accompanying the increase in pressure with depth in the Earth. It marks the transition from upper to lower mantle and implies major changes in density (Dziewonski and Anderson 1981), rheology (Stolper and Ahrens 1987; Williams and Jeanloz 1988; Karato et al. 1990), and chemistry (Kellogg et al. 1991; Tschauner et al. 1999). Although the Earth's mantle is dominated by mixed oxide silicates, the pure silica phases provide the basic model of this coordination change (e.g., Williams and Jeanloz 1988). Previous work on this transition has focussed on ambient temperatures. Low-pressure silica phases are initially compressed by tetrahedral tilt and collapse to dense, higher-coordinated structures by multiple reconstructive phase transitions into disordered sixfold coordinated phases based on corner-sharing octahedra (Tsuchida and Yagi 1990; Kingma et al. 1996; Haines et al. 2001; Dubrovinsky et al. 2001). This behavior differs from that of several structural analogues of silica that can be compressed into closed packed structures continuously (Haines et al. 2003). Because of kinetic barriers for Si-O bond reconstruction, diffusionless transitions are preferred. This type of mechanism appears to prevail to temperatures of 1200 K (Dubrovinsky et al. 2003). Here, we show that at the higher temperatures of the Earth's mantle, the transformation from four- to sixfold coordinated Si is essentially different, characterized by an intermediate polymorph built from chains of irregular face-sharing polyhedra with an intrinsic disorder of the Si positions that allows for energetically more favorable bond angles by keeping an effective fourfold coordination of Si residing in these polyhedra. The silica polymorph reported here is the first such phase shown to occur independent of structure and density of the starting material and the experimental technique. Transitional structures similar to the present one may dominate dense silicate melts, thus controlling their viscosity and buoyancy in the Earth's mantle. The present is the first detailed structural study of a hither to unknown silica polymorph synthesized in a shock experiment. Another remarkable aspect of its structure is a close geometric relation with the α-PbO_2 structure (scrutinyite-type), suggesting that a sequence of transitions via these two polymorphs enables transformation from ^{IV}Si to ^{VI}Si, even under conditions where both the new polymorph and the α-PbO_2 structure are metastable (Ohno et al. 2002), like in shocked meteorites where the peak pressures likely never exceeded 25 GPa. Our finding of a new intermediate structure therefore proposes a new explanation of the occurrence of post-stishovite phases in shocked meteorites (Sharp et al. 1999; El Goresy et al. 2000; Dera et al. 2002).

RESULTS

Shock-wave recovery experiments on quartz and coesite starting materials achieved peak pressures of about 54 and 57 GPa. Shock recovery experiments were conducted on Z-cut, single-crystal α-quartz and polycrystalline coesite. The coesite sample was synthesized from G-grade Corning silica glass in a graphite capsule with a Getting-type cubic anvil apparatus at Caltech. The sample was held at approximately 4.5 GPa and 1200 K for 2 hours before quenching and slow decompression. Density measured by toluene immersion on the actual sample used is consistent with pure coesite, and powder X-ray diffraction (XRD) examination of similar synthesis runs typically shows only coesite peaks. Doubly polished thin discs with parallel faces were created from quartz and coesite samples. Each disk was then encased in a stainless steel recovery chamber for planar shock loading. Tantalum flyer plates launched at 1.93 and 1.87 km/s imparted shocks into the sample chamber of quartz and coesite, respectively. As both

* E-mail: olivert@physics.unlv.edu

sample materials are of lower impedance than the stainless steel chamber, the shock reverberates within the sample cavity until peak pressures of approximately 57 and 54 GPa are achieved asymptotically for quartz and coesite, respectively. Temperatures achieved in shock-loaded quartz and coesite are estimated to be 1800–2200 K. The shocked materials were retrieved by cutting the container in half while cooling the saw blade and keeping the cutting speed as low as 1 mm/min. The sample was recovered from a lens shaped cavity within the container. In addition, we loaded a synthetic single crystal platelet of tridymite, about 30 μm in diameter and 5 to 10 μm thick, using pure H_2O ice as a pressure medium. The tridymite sample was synthesized and provided by N.Z. Boctor, Carnegie Institution of Washington. The ice was made from double-distilled water. Small chips of ice were placed in the sample chamber cooled down to below 273 K. The ice chips enclosed the tridymite crystal such that it was completely surrounded by ice when the cell was pressurized. The sample was pressurized to ~30 GPa and heated with a CO_2 laser to 1900 (±100) K. The H_2O pressure medium absorbs the laser radiation as well, melts in the central area of the sample chamber, and heats up to the same temperature as the sample. The conditions during the experiment were therefore fully hydrostatic and the temperature distribution in the surroundings of the silica sample was homogeneous. We quenched the sample after heating for 120 seconds. Infrared (IR) spectrometry at the U2 Beamline at the Natural Synchrotron Light Source (NSLS) on the run products from earlier, similar experiments did not reveal any indication of hydroxyl groups in these samples. We recovered the material for XRD studies at ambient conditions. Material recovered from the shock experiments showed grain sizes between 1 and 10 μm with no porosity evident in visible light microscopy. Micro-Raman spectroscopy revealed that most of the material was amorphous and exhibited broad bands known from densified silica glass (Sharp et al. 1999; Grimsditch 1986; Hemley et al. 1986) (Fig. 1d). A few 3–10 μm diameter grains yielded the Raman spectrum of a crystalline phase, characterized by strong peaks of small half width (Figs. 1a–1c). The spectra are dominated by two strong and sharp peaks at 708 and 809 cm^{-1}, and two strong and broad features centered at 1355 and 1600 cm^{-1}. The energy band below 500 cm^{-1} exhibits a complex peak structure. These grains had a higher index of refraction than the surrounding glass. The Raman spectra indicate that the same phase is present in the material formed from shocked quartz and coesite. Recently published Raman spectra of quartz laser-shocked to above 23 GPa exhibit features around 700, 800, and 1400 cm^{-1} (de Resseguier et al. 2003). These spectral features are much weaker and broader than the present and may represent structurally disordered states of the same material. We retrieved a few hundred micrograms of the shock-recovered coesite, mounted it on the tip of a borosilicate glass fiber, and exposed it to Mo$K\alpha_1$ radiation at 1.2 kW power. We collected the signal for 15 hours while oscillating the sample along φ within ±20°. We used a Rigaku Ultra-X rotating anode generator and a cylindrical image plate detector. The collected patterns exhibited diffraction fringes without radial variation in intensity distribution, and showed peaks of a crystalline phase along with a strong glassy background. The crystalline pattern is dominated by two low-angle peaks that are about ten times stronger than the next most intense diffraction peak. Four of the other observed peaks belong to steel, which can be attributed to the container material. Twenty peaks having relative intensities above 2% of the sample peak at 16.4 °2θ were assigned to a crystalline silica phase. We used the program Jade 6.5+ to index these peaks. We obtained nine fits to orthorhombic cells with dimensions of 2.5, 4.9, and 7.4 Å, which are very good to excellent by means of the number of observed reflections matched and the small deviations between calculated and observed spacings. Based on these cells, we could identify a further seven peaks below 30 °2θ of relative intensity 1 to 2% as belonging to the same phase, and we selected and refined two cells of symmetry *Pcn*2 and *Pmna*, which reproduce the observed *d*-spacings equally well. All but two reflections below 30 °2θ were observed. Besides those of the steel contamination, one unindexed reflection was observed. Above 30 °2θ it is hard to distinguish different reflections, but within the given angular resolution, the proposed cell matches the higher angle peaks as well (see Fig. 2a and insert). We also collected XRD signals for 12 hours on the sample retrieved from the DAC, and found that it exhibits the same XRD patterns as those from the shockwave experiments (Fig. 2b). The overall signal is two to three times weaker due to the much smaller sample size. Below 28 °2θ, we observed 14 of 19 reflections of the same phase as found in the shocked coesite sample and

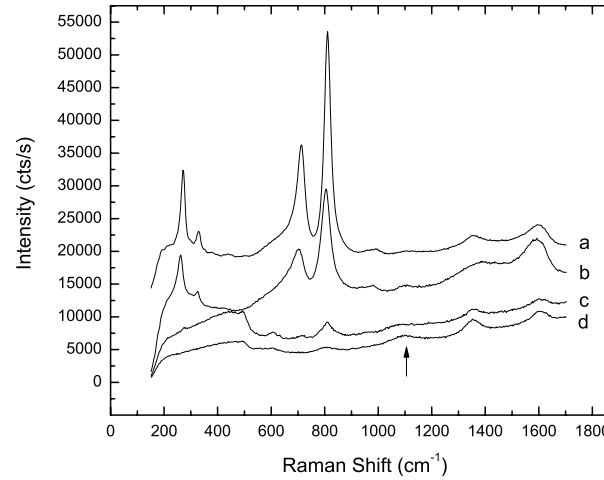

FIGURE 1. Raman spectrum of single grains of the crystalline phase recovered from shock-loaded coesite (**a**), shock-loaded quartz (**b**), and spectra from single grains of halfway and fully vitrified retrieved silica (**c**, **d**). The spectra of the crystalline phase clearly show the absence of Si-O tetrahedral stretching vibrations that would occur around 1100 cm^{-1}. The broad, intense peaks around 1350 and 1600 cm^{-1} match the 1st overtones of the strong Raman shifts at 708 and 809 cm^{-1}. Their high relative cross section and symmetric peak shape suggests, however, that there is a contribution from first-order scattering that can be assigned to Si-O bond stretching, which involves the disordered Si on the 8i site. Along with loss of structural order, the two peaks at 708 and 809 cm^{-1} lose intensity relative to the shifts around 1350 and 1600 cm^{-1} and a peak around 1060 cm^{-1}, characteristic of the Si-O tetrahedral stretch in silica glasses, rises (arrow). This change of relative intensity is consistent with vitrification controlled by unfolding of the polyhedral chains to tetrahedral networks thus reversing the tilt-compression mechanism proposed by Stolper and Ahrens (1995).

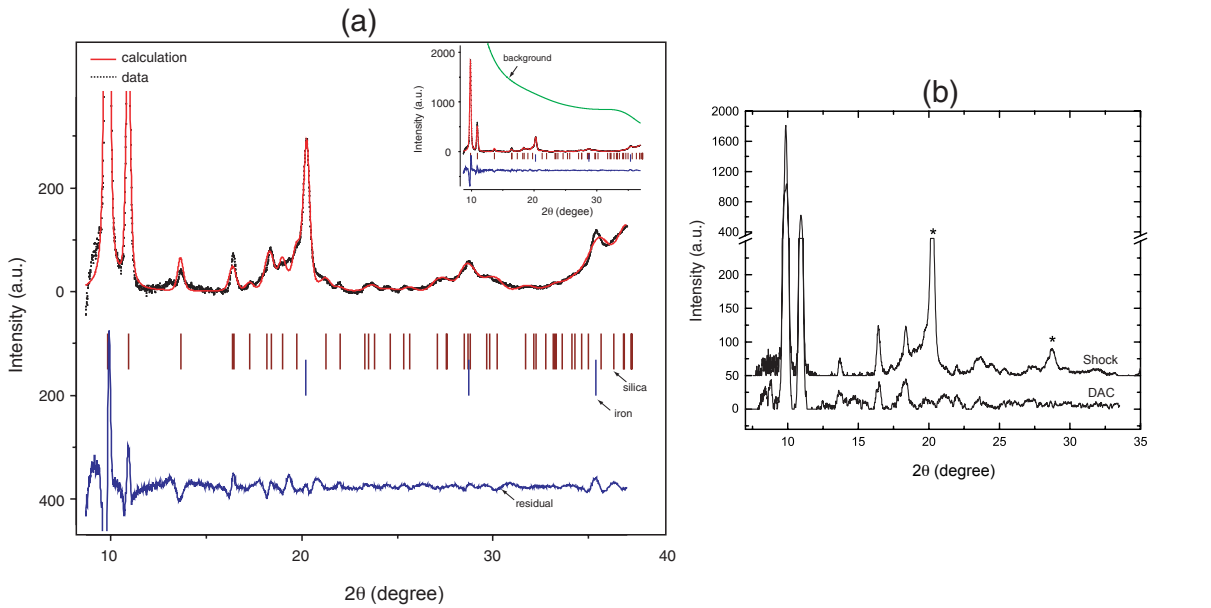

FIGURE 2. (**a**) Diffraction patterns of the material recovered from shock-loaded coesite between 12 and 35 °2θ and intensities up to 400 arbitrary unit (a.u.). A close match between the observed and refined calculated patterns, even for weak or overlapping peaks, is evident. The red curve indicates the calculated diffraction pattern. The black dotted curve denotes the observed pattern, and the blue curve the residual of the observation relative to calculation. Tick marks indicate the reflections of the calculated, refined cells of the *Pmna* silica phase and of stainless steel. The refined lattice parameter of the shocked stainless steel is 2.8600 Å. ***Inset***: The complete pattern showing the whole range of observed intensities. The green line denotes the fitted background. (**b**) Diffraction pattern of silica retrieved from a diamond-anvil cell after laser heating at ~30 GPa (lower curve, labeled as DAC) compared to the pattern of the material recovered from shock-loaded coesite (upper curve, labeled as Shock). Asterisks (*) indicate peaks from the stainless steel chamber for the shocked sample. Both patterns exhibit almost identical relative intensities of peaks indicating that both experiments yield the same phase.

refined the cell based on these reflections (Table 1). No additional reflections occur in this sample. A density slightly lower than that of the shock-recovered crystalline phase indicates the relative progress of vitrification in this sample (Table 1). The present phase cannot be preserved for long times at ambient conditions. Raman spectra collected over a period of two weeks show the decline of structural order. Vitrification of the shock-recovered material was complete after one month. As we will show now, the present phase represents a snapshot of the transformation of $^{IV}SiO_2$ to $^{VI}SiO_2$, but at ambient conditions (and probably at all conditions), is less stable than either the beginning or ending phases of this transformation.

DISCUSSION

The present phase does not match any of the known silica phases. The density is between 4.35 and 4.18 g/cm^3, which overlaps the 4.35 to 4.28 g/cm^3 range of stishovite and the known post-stishovite phases (Sharp et al. 1999; El Goresy et al. 2000; Dera et al. 2002), but the new structure does not represent any of the known structural forms occurring along the various transformation paths of post-stishovite phases (Haines and Leger 1997). The two strong, low-angle peaks suggest a strong anisotropy

TABLE 1. List of observed and calculated reflections below 30 °2θ

	Shocked coesite				Laser-heated tridymite in DAC		
No.	d_{obs} (Å)	d_{calc} (Å)	Δd(Å)	(*hkl*)	d_{obs} (Å)	d_{calc} (Å)	Δd(Å)
	esd:0.005				esd:0.005		
1	4.134	4.1382	0.004	011	4.104	4.1333	0.029
2	3.716	3.7274	0.011	020	3.699	3.7147	0.016
3	2.979	2.9830	0.004	021	2.992	2.9763	–0.016
4	2.485	2.4875	0.002	002	–	2.4871	–
5	2.485	2.4813	0.000	030	2.473	2.4765	0.004
6	2.357	2.3596	0.003	012	–	2.3585	–
7	2.255	2.2523	–0.002	101	2.282	2.2779	–0.004
8	2.223	2.2231	0.000	031	2.218	2.2169	–0.001
9	2.160	2.1560	–0.004	111	2.178	2.1781	–0.000
10	2.067	2.0691	0.002	022	2.066	2.0667	0.001
11	1.926	1.9277	0.002	121	1.939	1.9419	0.003
12	1.863	1.8637	0.001	040	1.858	1.8573	–0.001
13	1.759	1.7580	–0.001	032	–	1.7549	–
14	1.744	1.7453	0.001	041	–	1.7400	–
15	1.729	1.7243	–0.005	112	1.735	1.7353	0.000
16	1.673	1.6688	–0.005	131	1.677	1.6765	–0.001
17	1.615	1.6188	0.004	013	1.620	1.6183	–0.002
18	–	1.6006	–	122	–	1.6086	–
19	1.514	1.5152	0.001	023	1.513	1.5141	0.001
20	1.497	1.4915+ 1.4910	–0.006	042+ 050	–	1.4882+ 1.4859	– –
21	1.445	1.4429	–0.002	132	–	1.4479	–
22	–	1.4359	–	141	–	1.4395	–
23	1.428	1.4282	0.000	051	–	1.4237	–
24	1.393	1.3843	–0.006	103	–	1.3920	–
25	1.379	1.3794	0.000	033	1.378	1.3778	–0.000
26	1.360	1.3629	0.003	113	–	1.3682	–
27	1.230	1.2999	0.001	123	–	1.3035	–
28	1.285	1.2843	0.003	142	–	1.2869	–
29	–	1.2788	–0.006	052	–	1.2756	–
30	–	1.2630	–0.000	200	–	1.2625	–
31	1.242	1.2438+ 1.2425	0.003	004+ 060	–	1.2436+ 1.2382	–

Notes: The cell of the crystalline phase retrieved from the shockwave experiment assumes space group Pmna (53) and has dimensions of 2.526(50), 7.455(1), 4.975(1), V= 93.68 Å3, ρ = 4.26 (9) g/cm^3. The uncertainty in density results mostly from the large error in a-axis length. This is the axis, along which the disordered polyhedral chains run (see Fig. 3). This dimension is probably most affected by changes due to beginning vitrification. The refined cell (Pmna) of the sample from the diamond cell experiment has dimensions of 2.557(1), 7.430 (2), 4.982(1), V = 94.64 Å^3, ρ = 4.22 (1) g/cm^3.

of the structure. Pronounced diffraction peaks at similar angles also occur in cristobalite and tridymite, where they originate from scattering of planes normal to the hexagonal channels of silica tetrahedra. Based on this observation, we were able to postulate a starting model for the crystal-structure analysis. In this model, a sublattice formed from distorted hexagonal arrays of O atoms arranged in channels runs along the *a*-axis. The Si atoms have to reside off-center within these hexagonal arrays to establish covalent bonds with O, thereby creating chains running along the *a*-axis. We found that assigning two different positions to the Si atoms with partial occupancy yields a model with a diffraction pattern similar to that observed. We optimized this model based on the observed integrated intensities using the global and local optimization program Endeavour 1.1 (Putz et al.1999) at the Carnegie Institution of Washington with the kind permission of C.T. Prewitt. The *Pmna* cell gives a refinement factor for integrated intensities of 8.5% whereas the *Pcn*2 cell gives 17%. Therefore, we prefer the centrosymmetric cell (*Pmna*). We then used the structure factors of this optimized structure model for an F_{calc}-weighted refinement of the modeled diffraction pattern (Larson and von Dreele 1995). As shown in Figure 2a, the refined model pattern matches the observed one surprisingly well, including weak peaks whose intensities are only three- to four- times noise level. Our refinement yielded a χ^2 of 21.6 and a wRp of 0.0123 (0.029 after background subtraction). The number of observations was 2830. However, the poor statistics of most of the observed peaks do not allow for further meaningful refinement of the atomic coordinates. Cell dimensions and calculated and observed *d*-values down to 30 °2θ are listed in Table 1. We give the calculated fractional coordinates in the caption of Figure 3.

The principal aspects of the optimized model structure (Fig. 3) are quite novel. Silicon resides on two different positions of Wyckoff symmetries 4h and 8i with occupancies of 0.5 and 0.25, respectively. The Si on the 4h position has four neighboring O atoms within 1.5 to 2.2 Å and three second-nearest neighbors within 2.5 Å. The four shortest Si-O bonds establish a triangular pyramid with the Si atom residing in the basal plane to which the longest Si-O bond is perpendicular. Therefore, this SiO_4 unit is very different from the regular tetrahedron with Si at the center, which are present in ambient pressure silica. This is expected because, in silica, the Si-O tetrahedra are dynamically unstable at the pressures where the present phase formed (Stolper and Ahrens 1987; Williams and Jeanloz 1988; Hemley et al. 1986; Hazen et al. 1989; Wentzkovitch et al. 1998; Tse and Klug 1991; Chaplot and Sikka 1993). The faces of the $Si(4h)O_4$ pyramids and an additional O form a bipyramidal cage of six O atoms in which the Si(8i) positions are located. In each position, Si has four nearest neighbor O atoms within 1.4 to 2.0 Å to establish covalent Si-O bonds if the position is filled. The filling of these bipyramidal sites and the precise position of the Si atoms are constrained by the fact that unrealistic Si-O-Si bond angles <30° might arise

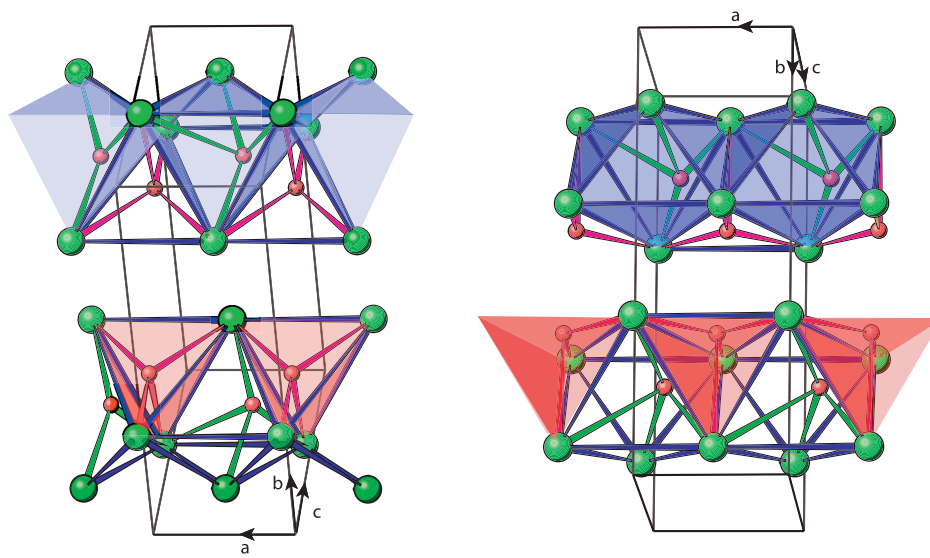

FIGURE 3. Structure representation of the new silica phase. Green spheres are O, red spheres are Si, red and green lines indicate Si-O bonds, and blue lines mark the edges of polyhedra. Two chains of SiO_2 run through each elementary cell along the ***a***-axis. The chains are built from alternating bipyramidal and triangular pyramidal units. In the upper chains the faces of the bipyramids are colored blue, whereas, in the lower ones, the faces of the pyramids are colored red. Figures 3a and 3b show two different choices of Si site occupancy. Clearly the relative rotation of both chains by 90° and their translation by *a*/2 can be seen. Because there is no general ordering of Si-positions on its two sites, these rotations and translations of chains induce inter-chain disorder. Beside this inter-chain disorder, there is a macroscopic degeneracy of Si on the 8i site as described in the text.

The calculated fractional coordinates are: Si(4h): 0.000, 0.347, 0.255; Si(8i): 0.177 – *x*, 0.215, 0.159 – *z*; O(4h): 0.000, 0.077, 0.382; O(4h): 0.000, 0.661, 0.105. The occupancy of the 4h site of Si is 0.5, and that of the 8i site is 0.25. *x* is between 0 and 0.15, *z* is between 0.00 and 0.08 Å. If the Si on the 8i position orders, *x* becomes zero and the cell symmetry reduces to a subgroup of *Pmna*.

between adjacent 8i sites with random 25% filling. Even so, if the Si atoms sit at the average atomic coordinates of the model structure, one Si(4h)-O-Si(8i) angle is as small as 40°. In order to avoid this unfavorable value, the actual atomic coordinates differ for each bipyramid from the measured average position (see caption of Fig. 3), thus maximizing this angle to between 60 and 70°. This variation of local atomic coordinates creates a macroscopic disorder, similar to the disordered proton positions in water ice but unlike the common sublattice disorder where atomic positions are random within given spatial constraints. We note that the displacement of Si from the center of a polyhedron formed by six O atoms to establish lower bond coordination resembles the only known case of a fivefold coordination of Si in a solid silicate (Angel et al. 1996). In that case, however, the Si position is determined uniquely and O-atom positions are displaced along with the Si position. We also note that the present phase displays a completely different state of transition between four- and sixfold coordinated silica than the proposed penta-phase (Badro et al. 1997).

The pyramidal and bipyramidal units form face-sharing chains running along the *a*-axis, thus establishing an extreme oxygen packing density along this direction. However, we recall that the Si positions are only partially occupied. The choice of sites occupied also determines the orientation of the chains along the ***a***-axis. For instance, in Figure 3a, the chains are rotated by 90° and translated by *a*/2 relative to the chains shown in Figure 3b. Hence, there is a macroscopic intra-chain disorder and an additional inter-chain disorder. Macroscopic disorder implies unusual material properties, e.g., a non-vanishing entropy at 0 K. It would be interesting to examine the properties of the present new silica phase in that respect. We tentatively assign the strong Raman peaks at 708 and 809 cm^{-1} to Si-O bond stretching in the pyramidal units. The bond distances of 1.9 ± 0.3 Å are in the range of distances found in stishovite (Kirfel et al. 2002), which has stretching vibrations in the same range of energies (Kingma et al. 1996). The broad and intense peaks at 1360 and 1600 cm^{-1} match the overtone of these vibrations in the absence of strong phonon dispersion. We observed the second overtone of these peaks, indeed. However, the relative cross section and symmetric shape of these peaks indicate that at least part of the scattering intensity results from first-order processes. The bond distances of disordered Si in the bipyramidal unit are in the range of 1.4 to 2.0 Å, with three bonds between 1.4 and 1.7 Å on average. The stretching vibration of these bonds probably contributes to the features around 1360 and 1600 cm^{-1}, and the broadness of these peaks results at least partially from the macroscopic disorder.

In the new polymorph, Si is not sixfold coordinated by O. It is extraordinary, therefore, that the density of this structure is in the range of the known octahedrally coordinated silica phases. This result implies that silica can collapse to high density through formation of distorted, face-sharing oxygen polyhedra in addition to the stable structures involving corner-shared octahedra. The structure of the present polymorph, based on face-sharing chains of two different kinds of irregular polyhedra with intrinsic disorder, is reminiscent of the transformation mechanism from four- to sixfold coordinated silica in glasses and liquids by tilt of chains of edge-sharing tetrahedra into face-sharing chains as proposed by Stolper and Ahrens (1987). Although consistent with spectroscopic observations and geometrically intriguing, the chains of face-sharing octahedra resulting from this mechanism yield energetically unfavorable Si-O-Si bond angles (Stolper and Ahrens 1987). The new silica polymorph, however, exhibits a macroscopic disorder of the Si(8i) positions, which reconciles less energetic, large bond angles with the principle of face-sharing polyhedra. The present new polymorph shows that a compression-mechanism dominated by tilt results in a structure having a density similar to stishovite. However, physical constraints on bond angles imply a macroscopic disorder of the Si positions. The subsequent transformation-steps toward sixfold coordinated phases have to involve bond reconstruction.

Because of the fundamental similarity between the present structure and the melt structure proposed by Stolper and Ahrens (1987), we suggest that transitional structures similar to the present one occur in dense silicate melts thus controlling their viscosity and buoyancy in the Earth's mantle. The conditions of formation of the present new polymorph match the metastable extension of the transitional *P-T* region between four- and sixfold coordinated silica melt. The present polymorph forms at 30 GPa, 1800 K within the stability field of stishovite and extends into the stability field of $CaCl_2$-type silica at 57 GPa (Ono et al. 2002; Murakami et al. 2003). We interpret the recently reported Raman spectra of quartz laser shocked to above 23 GPa (de Resseguier et al. 2003) as an indication that the present phase forms at pressures as low as 23 GPa. The pressure range from ~ 20 to 60 GPa includes the range of strong curvature of the melting curve of stishovite (Shen and Lazor 1995), which corresponds to a transitional regime in the melt structure. We note that such metastable polymorphs have not been found in longer-term, static-heating experiments under these conditions in either silica (Dubrovinski et al. 2001; Ono et al. 2002; Murakami et al. 2003) or GeO_2 (Prakapenka et al. 2003), thus affirming the transitional character of the present polymorph.

SUMMARY REMARKS

In the present work, we have shown that quartz and coesite under shock-wave loading to ~56 GPa, and tridymite after short-term laser heating in diamond cells at ~30 GPa under hydrothermal conditions, all transform into the same crystalline polymorph. These starting phases have densities ranging from 2.2 to 2.9 g/cm^3, thus covering the full range of densities of tetrahedrally coordinated silica phases. Hence, the present new polymorph apparently forms independent of the initial density of the tetrahedral starting material. This transformation also occurs during two very different types of short-timescale experiments. Furthermore, it is remarkable that the new polymorph forms out of silica phases with such different framework arrangements of the SiO_4 tetrahedra as, e.g., tridymite and coesite. All this indicates that the new silica structure may play a general role in transformations of silica phases from tetrahedrally to octahedrally coordinated networks. A close structural relation between the new polymorph and a-PbO_2 silica can be found by mapping of the atomic positions with sublattice rotations and translations (see appendix 1). We therefore infer that there may be a general pathway for the transformation of $^{IV}SiO_2$ to the a-PbO_2 structure and, thereafter, to other octahedral silica phases with the present crystalline structure as an intermediate product, and with the

density increase occurring before the formation of a fully sixfold coordinated phase. We also note that the new polymorph was found in our laser-heating experiments at a pressure as low as 30 GPa, which is within the stability field of stishovite. This finding suggests that, in addition to possible roles of chemical impurities (Sharp et al. 1999; El Goresy et al. 2000) and of formation in high-temperature shear-concentration bands (Grady 1974; Tan and Ahrens 1990), it is conceivable that the transformation path involving the new structure can explain the observation of a-PbO_2 and baddeleyite-structured silica as metastable phases in shocked meteoritic material (Sharp et al. 1999; El Goresy et al. 2000; Dera et al. 2002) where peak pressures probably did not exceed 25 GPa (Sharp et al. 2003), i.e., at pressures where stishovite is known to be the stable phase of silica and 20 GPa (Dubrovinsky et al. 2001) to 60 GPa (Ono et al. 2002) below the experimental detection of such phases. This scenario is consistent with the observation of the α-PbO_2 type as metastable structure in GeO_2 (Prakapenka et al. 2003) and the large *P-T* range of experimental observation of α-PbO_2-type silica along with the observation of the $CaCl_2$-type silica (Dubrovinski et al. 2001; Ono et al. 2002; Murakami et al. 2002).

Further studies are needed to confirm the general significance of this mechanism in silica, as well as the existence of similar mechanisms of transformation and analogous intermediate phases with pyramidal coordination polyhedra in mixed oxide silicates and other materials that undergo pressure-induced changes in cation coordination from tetrahedral to octahedral.

ACKNOWLEDGMENTS

This work was supported by NSF Grant EAR-0207934 and NASA Grant NAG5-10198. S.N.L. was also sponsored by a Director's Post-doctoral Fellowship at Los Alamos National Laboratory (P-24 and EES-11). O.T. also acknowledges support from NNSA Cooperative Agreement DE-FC88-01NV14049. We appreciate the help of G.R. Rossman and E. Arredondo in Raman spectroscopy, P. Dera, C. Prewitt, R.J. Hemley, and H.K. Mao for kind permission to use their X-ray diffraction and CO_2-laser heating facilities. We thank P.Dera and two anonymous reviewers for helpful comments. Contribution no. 8943, Division of Geological and Planetary Sciences, California Institute of Technology.

REFERENCES CITED

Angel R.J., Ross, N.L., Seifert, F., and Fliervoet, T.F. (1996) Structural characterization of pentacoordinate silicon in a calcium silicate. Nature, 384, 441–444.

Badro, J., Teter, D.M., Downs, R.T., Gillet, P., Hemley, R.J., and Barrat, J.-L. (1997) Theoretical study of a five-coordinated silica polymorph. Physical Review B, 56, 5797–5806.

Chaplot S.L. and Sikka, S.K. (1993) Molecular-dynamics simulation of pressure-induced crystalline-to-amorphous transition in some corner-linked polyhedral compounds. Physical Review B, 47, 5710–5714.

Dera, P., Prewitt, C.T., Boctor, N.Z., and Hemley, R.J. (2002)Characterization of a high-pressure phase of silica from the Martian meteorite Shergotty. American Mineralogist, 87, 1018–1023.

de Resseguier, T., Berterretche, P., Hallouin, M., and Petitet, J.P. (2003) Structural transformations in laser shock-loaded quartz. Journal of Applied Physics 94, 2123–2129.

Dubrovinsky, L.S., Dubrovinskaia, N.A., Prakapenka, V., Seifert, F., Langenhorst, F., Dmitriev, V., Weber, H.P., and Le Bihan, T. (2003) High-pressure and high-temperature polymorphism in silica. High Pressure Research 23, 35–39.

Dubrovinsky, L.S., Dubrovinskaia, N.A., Saxena, S.K., Tutti, F., Rekhi, S., Le Bihan, T., Shen, G.Y., and Hu, J. (2001)Pressure-induced transformations of cristobalite. Chemical Physics Letters, 333. 264–270.

Dziewonski, A.M. and Anderson, D.L. (1981) Preliminary Reference Earth Model. Physics of the Earth and Planetary Interiors, 25, 297–356.

El Goresy, A., Dubrovinsky, L., Sharp, T.G., Saxena, S.K., and Chen, M. (2000) A monoclinic post-stishovite polymorph of silica in the Shergotty meteorite. Science, 288, 1632–1634.

Grady, D.E. (1974) Shock deformation of brittle solids, Journal of Geophysical Research, 85, 913–924.

Grimsditch, M. (1986) Polymorphism in amorphous SiO_2. Physical Review Letters, 52, 2379–2381.

Haines, J. and Léger, J.M. (1997) X-ray diffraction study of the phase transitions and structural evolution of tin dioxide at high pressure. Physical Review B, 55, 11144–11154.

Haines, J., Léger, J.M., Gorelli, F., and Hanfland, M. (2001) Crystalline post-quartz phase in silica at high pressure. Physical Review Letters 87, 155503–1155503-4.

Haines, J., Chateau, C., Léger, L.M., Bogicevic, C., Hull, S., Klug, D.D., and Tse, J.S. (2003) Collapsing cirstobalitelike structures in silica analogues at high pressure. Physical Review Letters 91, 015503-1–015503-4.

Hazen, R.M., Finger, L.W., Hemley, R.J., and Mao, H.K. (1989) High-pressure crystal-chemistry and amorphization of alpha-quartz. Solid State Communications, 72, 507–511.

Karato, S. Fujino, K., and Ito, E. (1990) Plasticity of $MgSiO_3$ Perovskite—The results of microhardness tests on single crystals. Geophysical Research Letters, 17, 1.

Kellogg, L.H., Hager, B.H., and van der Hilst, R.D. (1991) Compositional stratification in the deep mantle. Science, 283, 1881–1884.

Kingma, K.J., Cohen, R.E., Hemley, R.J., and Mao, H.K. (1995) Transformation of stishovite to a denser phase at lower-mantle pressures. Nature 374, 243–245.

Kingma, K.J., Mao, H.K., and Hemley, R.J. (1996) Synchrotron X-ray diffraction of SiO_2 to multimegabar pressures. High Pressure Res. 14, 363–374.

Kirfel, A., Krane, H.G., Blaha, P., Schwarz, K., and Lippmann, T. (2001) Electron-density distribution in stishovite. Acta Crystallographica A 57, 663–677.

Larson, A.C. and von Dreele, R.B. (1995) General Structure Analysis Software (GSAS), LAUR 86–748, Los Alamos National Laboratory, NM, USA.

Murakami, M., Hirose, K., Ono, S., and Ohishi, Y. (2003) Stability of $CaCl_2$-type and α-PbO_2-type SiO_2 at high pressure and temperature determined by in-situ X-ray measurements. Geophysical Research Letters, 30, 1207.

Ono, S., Hirose, K., Murakami, M., and Ishiki, M. (2002) Post-stishovite phase boundary in SiO_2 determined by in situ X-ray observations. Earth and Planetary Science Letters, 197, 187–192.

Putz, H., Schön, J.C., Jansen, M. (1999) Combined method for ab initio structure solution from powder diffraction data. Journal of applied crystallography 32, 864–870.

Sharp, T.G., El Goresy, A., Wopenka, B., and Chen, M. (1999) A post-stishovite SiO_2 polymorph in the meteorite Shergotty: Implications for impact events. Science, 284, 1511–1513.

Sharp, T.G., Xie, Z., Aramovich, C., and DeCarli, P.S. (2003) Pressure-temperature histories of shocked-induced melt veins in chondrites. Lunar & Planetary Science 34, Abstract no. 1278.

Shen, G.Y. and Lazor, P. (1995) Measurements of melting temperatures of some minerals under lower mantle pressures. Journal of Geophysical Research 100, 17699–17713.

Stokes, H.T. and Hatch, D.M. (2002) Procedure for obtaining microscopic mechanisms of reconstructive phase transitions in crystalline solids. Physical Review B, 65, art. no.144114.

Stolper, E.M. and Ahrens, T.J. (1987)On the nature of pressure-induced coordination changes in silicate melts and glasses. Geophysical Research Letters, 14, 1231.

Tan, H. and Ahrens, T.J. (1990) Shock-induced polymorphic transitions in quartz, carbon, and boron-nitride. Journal of Applied Physics, 67, 217–224.

Tolédano, P. and Tolédano, J.C. (1976) Order-parameter symmetries, Physical Review B, 16, 386–407.

—— (1982) Nonferroic phase transitions. Physical Review B, 25, 1946–1964.

Tschauner, O., Zerr, A., Specht, S., Rocholl, A., Boehler, R., and Palme, H.(1999) Partitioning of nickel and cobalt between silicate perovskite and metal at pressures up to 80 GPa. Nature, 398–607, 604.

Tse, J.S. and Klug, D.D. (1991) Mechanical instability of alpha-quartz - a molecular-dynamics study. Physical Review Letters, 67, 3559–3562.

Tsuchida, Y. and Yagi, T. (1990) New pressure-induced transformations of silica at room-temperature. Nature, 347, 267–269.

Williams, Q. and Jeanloz, R. (1988) Spectroscopic evidence for coordination changes in silicate glasses and melts. Science, 239, 902–905.

Wentzcovitch, R.M., da Silva, C., Chelikowsky, J.R., and Binggeli, N. (1998) A new phase and pressure induced amorphization in silica, Physical Review Letters, 80, 2149–2152.

MANUSCRIPT RECEIVED AUGUST 5, 2003
MANUSCRIPT ACCEPTED NOVEMBER 17, 2003
MANUSCRIPT HANDLED BY ROBERT DYMEK

(see Appendix on next page)

APPENDIX 1: STRUCTURAL RELATIONSHIP BETWEEN THE NEW SiO_2 PHASE AND α-PbO_2-TYPE SILICA

This appendix documents close structural relationship between the newly discovered dense SiO_2 phase and the α-PbO_2 (scrutinyite)-type structure of SiO_2. This structural relation implies existence of a simple transformation mechanism. Both phases have similar densities [4.26(9) and 4.31(2) g/cm^3 (Dera et al. 2002)]. The cell dimensions of the present phase relate to those of α-PbO_2-type silica by a doubling of the short axis and a shortening of the other two axes, thus keeping the cell volume for both phases approximately equal (see the table below). The transformed cell belongs to space group *Pbcn*. Without inferring the detailed transformation mechanism, we show close structural relation of the present new phase and α-PbO_2-type silica by mapping the atomic positions of the former onto the latter. The conclusion that the structures have a close structural relation and are connected by a simple transformation pathway is based on the fact that this mapping is by simple rotations and translations of sublattices (a common characteristic of related structures, which certainly holds in case of structures immediately related by group-subgroup relations (see e.g., P.Toledano and J.C. Toledano 1977, 1982), but it also holds for related structures where such direct algebraic relation does not exist (e.g., Stokes and Hatch 2002).

In the table we list the details of these mathematical transformations and give the atomic coordinates of the resulting α-PbO_2-type structure. Its atomic coordinates closely match those of α-PbO_2-type silica found in the Shergotty meteorite (Dera et al. 2002).

The following is a tabular overview of the mapping of the present phase onto α-PbO_2-type silica, involving pure axis transformation from space group *Pmna* to *Pbcn*, and subsequent rotation and relative translation of atoms. Column 2 shows the Si- and O- coordinates for the present new phase (*Pmna*). Axis transformation from *Pmna* to *Pbcn* yields the atomic coordinates in Column 3. Subsequent rotation (Column 4) and translation (Column 5) yield atomic coordinates (Column 6) equivalent to those of α-PbO_2 silica (Column 7). These transformations map the two originally distinct, partially occupied Si positions (Si1 and Si2) onto one fully occupied 4c position, and the two O positions onto one general position in the α-PbO_2 cell. All rotations involve 90° and 180° angles only, and the translation vectors involve displacements by 1, 2, and 4 times 1/16 of an axis length.

APPENDIX TABLE 1.

Atom	Pmna Coord. in Å	Pbcn* Coord. in Å	Rotation of coordinates	Subsequent Translation	Calculated coordinates (Å)	α-PbO_2-type silica† (Å)
Si1 (8i)	$\begin{pmatrix}0.177\\0.215\\0.159\end{pmatrix}$	$\begin{pmatrix}0.159\\0.354\\0.0375\end{pmatrix}$	$\begin{pmatrix}0&0&1\\1&0&0\\-1&1&1\end{pmatrix}$	$\begin{pmatrix}0\\0\\0\end{pmatrix}$	$\begin{pmatrix}0.0375\\0.159\\0.2325\end{pmatrix}$	$\begin{pmatrix}0\\0.152\\0.250\end{pmatrix}$
Si2 (4h)	$\begin{pmatrix}0\\0.347\\0.255\end{pmatrix}$	$\begin{pmatrix}0.255\\0\\0.347\end{pmatrix}$	$\begin{pmatrix}0&1&0\\-1&0&1\\1&0&0\end{pmatrix}$	$\begin{pmatrix}0\\1/16\\0\end{pmatrix}$	$\begin{pmatrix}0\\0.155\\0.255\end{pmatrix}$	
O1 (4h)	$\begin{pmatrix}0\\0.0767\\0.382\end{pmatrix}$	$\begin{pmatrix}0.3824\\0\\0.0767\end{pmatrix}$	$\begin{pmatrix}1&1&0\\0&0&1\\1&0&0\end{pmatrix}$	$\begin{pmatrix}-1/8\\1/16\\0\end{pmatrix}$	$\begin{pmatrix}0.257\\0.139\\0.382\end{pmatrix}$	$\begin{pmatrix}0.234\\0.125\\0.419\end{pmatrix}$
O2 (4h)	$\begin{pmatrix}0\\0.661\\0.105\end{pmatrix}$	$\begin{pmatrix}0.105\\0\\0.6615\end{pmatrix}$	$\begin{pmatrix}1&1&0\\1&0&0\\0&0&1\end{pmatrix}$	$\begin{pmatrix}1/8\\0\\-1/4\end{pmatrix}$	$\begin{pmatrix}0.230\\0.105\\0.412\end{pmatrix}$	

* Axis transformation between the *Pmna*- and the *Pbcn*-cell is by $\begin{pmatrix}0&0&1\\2&0&0\\-1&1&0\end{pmatrix}$.

† Dera et al. (2002).